Biomedical Signal Processing and Control 20 (2015) 24–34

Contents lists available at ScienceDirect

Biomedical Signal Processing and Control

journal homepage: www.elsevier.com/locate/bspc

SEMG-based prediction of masticatory kinematics in rhythmic clenching movements

Hadi Kalani[a,b], Sahar Moghimi[a,c,*], Alireza Akbarzadeh[a,b]

[a] Center of Excellence on Soft Computing and Intelligent Information Processing, Ferdowsi University of Mashhad, Mashhad, Iran
[b] Mechanical Engineering Department, Ferdowsi University of Mashhad, Mashhad, Iran
[c] Electrical Engineering Department, Ferdowsi University of Mashhad, Mashhad, Iran

ARTICLE INFO

Article history:
Received 26 October 2014
Received in revised form 18 February 2015
Accepted 2 April 2015

Keywords:
Mastication
Surface electromyography (SEMG)
Kinematic parameters
Genetic algorithm (GA)
Time-delayed artificial neural network (TDANN)

ABSTRACT

This paper investigated the ability of a hybrid time-delayed artificial neural network (TDANN)/autoregressive TDANN (AR-TDANN) to predict clenching movements during mastication from surface electromyography (SEMG) signals. Actual jaw motions and SEMG signals from the masticatory muscles were recorded and used as output and input, respectively. Three separate TDANNs/AR-TDANNs were used to predict displacement (in terms of position/orientation), velocity, and acceleration. The optimal number of neurons in the hidden layer and total duration of delays were obtained for each TDANN/AR-TDANN and each subject through a genetic algorithm (GA). The kinematic modeling of a human-like masticatory robot, based on a 6-universal-prismatic-spherical parallel robot, is described. The structure and motion variables of the robot were determined. The closed-form solution of the inverse kinematic problem (IKP) of the robot was found by vector analysis. Thereafter, the framework for an EMG-based human mastication robot interface is explained. Predictions by AR-TDANN were superior to those by TDANN. SEMG signals from mastication muscles contained important information about the mandibular kinematic parameters. This information can be employed to develop control systems for rehabilitation robots. Thus, by predicting the subject's movement and solving the IKP, we provide applicable tools for EMG-based masticatory robot control.

1. Introduction

The significance of the chewing process on digestion and health necessitates studies of the mastication system. Mastication in humans consists of two basic movements, clenching and grinding. For clenching, the mandible moves in the sagittal plane; for grinding, it traces a circular path in the frontal plane. More than 20 muscles are involved in the process of human mastication, with six of them playing the major role in mandible control during coordinated masticatory movements [40,45]. These muscles are the temporalis muscles, attached from the side of the skull to the top of the mandible; the masseter muscles, attached between the cheek and the lower rear section of the mandible; the medial pterygoid muscles, attached to the inside of the skull and the mandible; the lateral pterygoid muscles, horizontally attached between the skull and the mandible; and the digastric muscle, attached between the skull and the chin. The masseter and temporalis muscles are primarily employed during clenching, whereas the pterygoid muscles have their main role during grinding. During jaw closing, the mandible is elevated by the temporalis and masseter muscles, while it is protruded by the masseter muscles. Pterygoid muscles protrude the mandible, produce its side-to-side movements, and generate the grinding motion.

Researchers have utilized various methods to study the chewing process, including gnathosonics for measuring the sounds of mastication, ultra-high-speed cinematography for measuring mandibular movement and velocity, and laryngophone for monitoring swallowing [15]. Small markers or magnets have been used to record the chewing trajectory [43,17]. Electromyography (EMG) has been employed to study changes in the electrical activity of the muscles during mastication [15,36,26,20]. Changes in EMG parameters are better able to assess the sensory characteristics than mechanical measurements [15]. Experimentally obtained signals, together with the physiological cross-sectional area of the muscles, have been employed to estimate instantaneous muscle forces [4,31] or to differentiate food-texture characteristics [15].

* Corresponding author at: Department of Electrical Engineering, Ferdowsi University of Mashhad, Mashhad 9177948974, Iran. Tel.: +98 5118805130; fax: +98 511 8763302.
E-mail address: s.moghimi@um.ac.ir (S. Moghimi).

http://dx.doi.org/10.1016/j.bspc.2015.04.003
1746-8094/

Additionally, EMG has been used to identify differences in chewing patterns between individuals and to classify individuals into groups according to their chewing efficiency [21,5–7].

Recently, EMG signals recorded from the muscles have been applied to control and classify the motion of prosthetic limbs [14], wheelchairs, and teleoperated robots [8,30,16,46,13,38,19]. Indeed, there have been various attempts to classify different movements for the purpose of controlling prostheses. Methods that have been applied to classify motions and categorize the mastication process include autoregressive (AR) models [16], Bayesian classifiers [22], artificial neural networks [25,18,41,42], fuzzy neural networks [3], dynamic recurrent neural networks [10], probabilistic neural networks [13,9], and Bayesian networks [8]. For instance, Graupe et al. [16] used an AR model to extract features from EMG signals and determine motions [47]. Au et al. [2] found that a time-delayed artificial neural network (TDANN) was capable of predicting shoulder and elbow motions from only EMG signals.

EMG signals are nonstationary. The feature patterns vary significantly depending on the tasks and conditions of the users. In addition, EMG signals are very likely to be affected by artifacts and noise. In practical applications, it is difficult to achieve sufficient accuracy and stable performance of motion classification when using only EMG signals. This achievement requires the careful operation of a prosthetic device or human-assisting manipulator. However, predicting the trajectory can be very helpful for guiding prosthetic devices in space. Toward this endeavor, a dentist-guided masticatory robot was recently developed for training patients with jaw disorders [39].

This study aimed to predict the kinematic parameters of motion during jaw opening and closing using surface EMG (SEMG) signals. Because surface electrodes are only able to record the electrical activities of the bilateral masseter and temporalis muscles, this paper focused on clenching movement. For motion prediction, a hybrid TDANN/auto-regressive TDANN (AR-TDANN) was developed from the experimental results. Predicted trajectory parameters were applied in a case study, to solve the inverse kinematic problem (IKP) and to estimate variations in the actuators (muscles) during jaw opening/closing. These findings will provide tools to control masticatory robots using SEMG signals.

The rest of the paper is organized as follows. The experimental setup, protocol, and hybrid algorithm are explained in Section 2. Kinematics of the masticatory robot and the hybrid motion framework for the SEMG-based human mastication robot interface are discussed in Section 2.4. The performance of the TDAAN/AR-TDANN in predicting the kinematic parameters of motion is presented in Section 3. This section also provides the results from solving the IKP problem, based on the predicted time-varying moments for one subject. A discussion and some remarks on future works are presented in Sections 4 and 5.

2. Materials and methods

2.1. Experimental setup

An 8-channel EMG system, with a sampling rate of 1 kHz, was used for recording the electrical activity of muscles (SEMG). For each subject, SEMG signals were recorded from four muscles: namely, the bilateral masseter and temporalis muscles (Fig. 1a). Surface electrodes were placed ~2 cm apart, oriented parallel to the muscle fibers, between the belly of each muscle and its end. Recorded raw SEMG signals were passed through a bandpass (15–400 Hz) 3rd order Butterworth filter [12]. A notch filter (50 Hz) was used to eliminate power line noise. The resulting signals were rectified and smoothed by a moving average window of size 200. The sampling rate of the preprocessed SEMG signals was reduced to 250 Hz, to match the sampling rate of the motion data. The *z*-scores of the processed signals were computed and used for further processing.

To trace the chewing trajectory, the Simi Reality Motion System (GmbH, Germany) was employed. Recorded data were preprocessed before modeling, using the Simi Motion software (Website: www.simi.com). The camera output was digitized to 250 frames per second (fps). Frequencies above 7 Hz were removed. To track the jaw motion, six small reflective markers, ~10 mm in diameter, were placed at specific facial locations (Fig. 1). Forehead markers were used as reference points.

2.2. Experimental protocol

We recruited seven volunteers (four males, age: 23 ± 2 years) for this study. All subjects were well-informed about the procedure and provided written consent to the experimental protocol. Subjects were seated in a comfortable chair and instructed to sit still during recording sessions. They were unable to view the computer screen. Each experiment consisted of six repeated trials. In each trial, subjects were asked to perform a symmetrical maximum voluntary mandible opening and closing in the sagittal plane (Fig. 2) within an interval of 5 s without the chin deviated toward the right or left side.

2.3. Genetic algorithm (GA) & TDANN

2.3.1. TDANN structure

A schematic of the TDANN used in this study is shown in Fig. 3. Nodes of the first hidden layer had log-sigmoidal transfer functions, and nodes of the output layer had purely linear transfer functions. Different delays of SEMG signals from the temporalis and masseter muscles were used as inputs. Kinematic variables (i.e., position, linear velocity, and acceleration of the chin point (CP) along the *x*- and

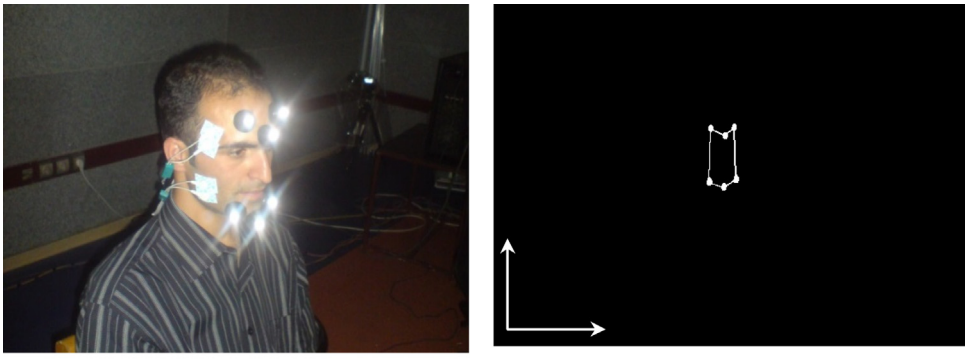

(a) (b)

Fig. 1. (a) Marker position on the subject's face. (b) Two-dimensional reconstruction of the marker set.

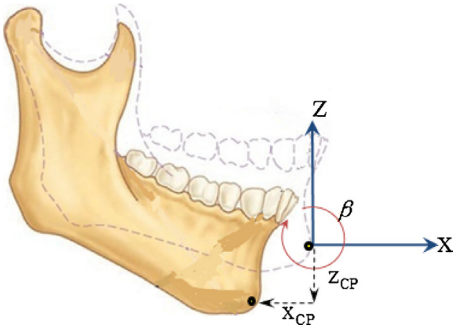

Fig. 2. View of clenching in the sagittal plane.

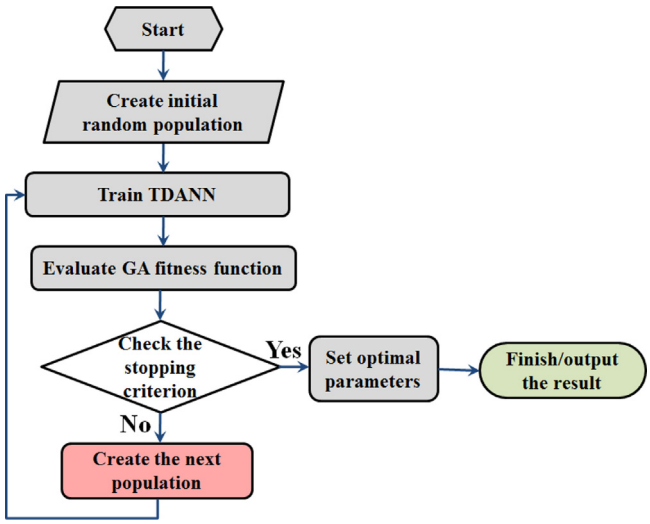

Fig. 4. Block diagram of the proposed technique.

z-axes, and the angle, angular velocity, and acceleration about y-axis) were set as outputs. Velocity and acceleration variables were determined by calculating the first and second derivatives of the trajectory related curves. Three TDANNs were trained for predicting the position/orientation (χ_{CP}, Z_{Cp}, β), velocity ($\dot{\chi}_{CP}, \dot{Z}_{Cp}, \dot{\beta}$), and acceleration ($\ddot{\chi}_{CP}, \ddot{Z}_{Cp}, \ddot{\beta}$) kinematic parameters, respectively.

Additionally, we proposed an AR-TDANN for better prediction of the kinematic variables. In this scenario, different delays of output variables were fed back to the system (Fig. 3) and used for predicting the current output values. Weights and biases of the network were initialized with random values. Batch training was used, in which the weights between the neurons were updated only after all of the training samples were exposed to the network. The Levenberg–Marquardt method [44], which gave the best possible results, was used for training.

2.3.2. Choice of TDANN structural parameters

The optimal number of neurons in the hidden layer and total duration of delays used for SEMG inputs were determined by a GA. The role of the GA was to find the best reference input and number of neurons for the prediction process. The TDANN (AR-TDANN) searched for the best nonlinear mapping function to predict the targets (kinematics variables), based on the schematic provided by the GA. The number of neurons in the hidden layer and the total delay were restricted to 10–60 and 0–1000 ms (with 200-ms intervals), respectively.

To obtain the best possible results, a fitness function was defined from the prediction error of the neural network, as follows:

$$F = \alpha||y - \hat{y}|| + \max(y - \hat{y}) + \beta \mathrm{std}(y - \hat{y}) \quad (1)$$

where y and $\hat{y}$ represent the measured and estimated output vectors, respectively. α and β were chosen empirically and added to balance the variation range of different terms on the right-hand side of Eq. (1). Three GA operators (selection, crossover, and mutation) led to a near-optimal solution through iterative computation. The crossover fraction was set to 0.8. Fig. 4 illustrates the proposed training algorithm.

Optimal parameters of TDANN/AR-TDANN were separately computed for each subject. After the optimal networks were found, three evaluation criteria were used to validate the trained networks: namely, the relative mean square error (RMSE),

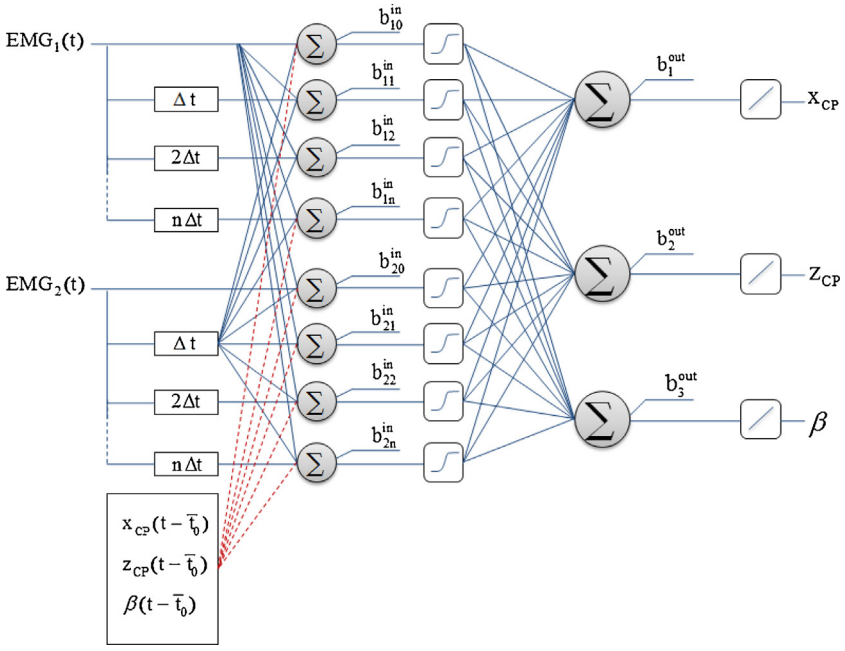

Fig. 3. Structural diagram of the TDANN (solid lines) and AR-TDANN (solid and dashed lines). $\bar{t}_0 = 50$, 100, or 150 ms.

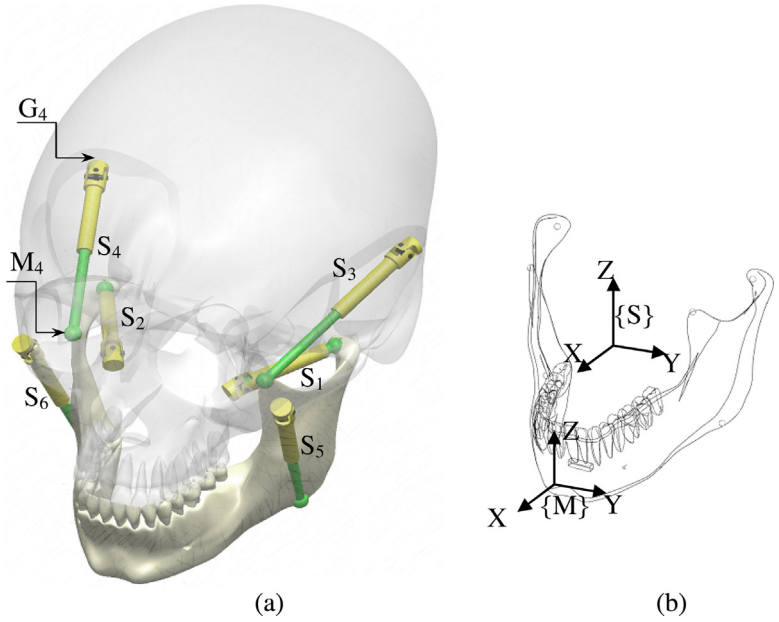

Fig. 5. (a) Mandible, actuators, and connecting points. (b) Schematic representation of the skull, mandible, and corresponding reference coordinate systems.

cross-correlation (CC), and average absolute error (AAE). The equations for these parameters are given below [33].

$$\text{RMSE} = 100 * \frac{\sum_i (y_i - \hat{y}_i)^2}{\sum_i (y_i)^2} \tag{2}$$

$$\text{CC} = 100 * \frac{\sum_i (y_i * \hat{y}_i)}{\sqrt{\sum_i (y_i)^2}\sqrt{\sum_i (\hat{y}_i)^2}} \tag{3}$$

$$\text{AAE} = \frac{\sum_i |y_i - \hat{y}_i|}{n} \tag{4}$$

where n is the number of samples. CC is a measure of similarity between y and $\hat{y}$, regardless of scaling. The proposed system was trained with 50% of the recorded data, while validation was performed with 50% of the data.

2.4. SEMG-based kinematic prediction

The primary motivation of this section is to determine whether sufficient information could be extracted from the SEMG signals of mastication muscles to control a masticatory robot. For this purpose, we solved the IKP, using the predicted kinematic parameters of motion from the SEMG signals. To represent the geometry of human mastication, we used a general 6-universal-prismatic-spherical (UPS) Stewart-Gough platform. The mobile and stationary platforms represent the human mandible and skull, respectively, and the actuators represent the jaw muscles (schematic in Fig. 5). Dimensions were chosen according to the available literature [45]. Actuators S_1 to S_6 in Fig. 5(a) represent the lateral pterygoid, temporalis, and masseter muscles, respectively. G_i and M_i ($i = 1, 2 \ldots 6$) represent the connecting locations of these muscles to the skull and mandible. Two coordinate systems, $\{\mathbf{S}\}$ and $\{\mathbf{M}\}$, are attached to the skull and mandible.

We used vector algebra to obtain the closed-form equations for the kinematics of the human-like masticatory robot. The configuration of the masticatory robot is specified by the position and orientation of the system $\{\mathbf{M}\}$ with respect to $\{\mathbf{S}\}$ (Fig. 6). For each leg, a vector loop equation can be written as,

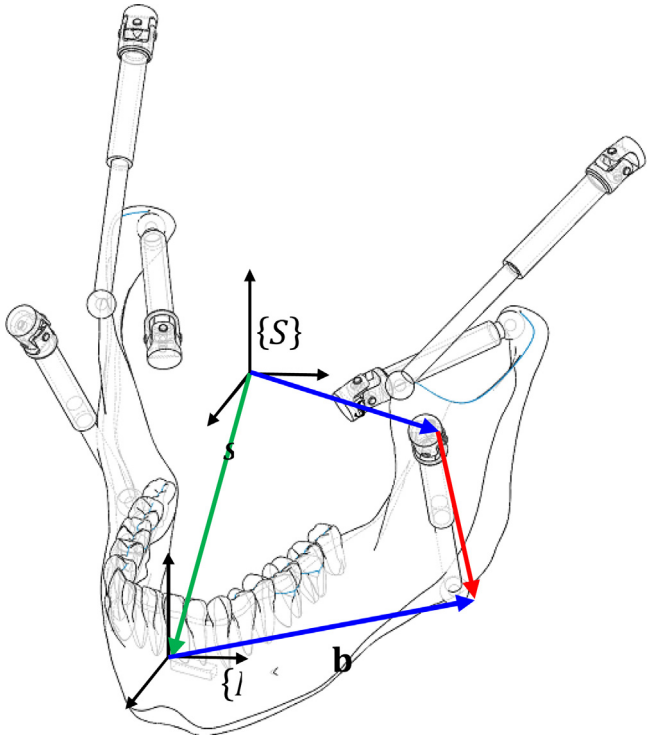

Fig. 6. Schematic diagram of the 6-UPS masticatory robot.

$$^{S}\mathbf{a}_i + {}^{S}\mathbf{s}_i = {}^{S}\mathbf{P} + {}^{S}_{M}\mathbf{R}\,{}^{M}\mathbf{b}_i \quad (i = 1,\ 2,\ \ldots,\ 6) \tag{5}$$

where $^{S}\mathbf{P}$ and $^{S}\mathbf{a}_i$ are the position vectors of the CP and mandible joint with respect to the skull coordinate system, respectively, and $^{M}\mathbf{b}_i$ represents the position vector of the skull joint with respect to the mandible coordinate system. The magnitude of $\mathbf{s}_i$ represents the actuated muscle length. The orientation of the mandible system $\{\mathbf{M}\}$ with respect to the skull coordinates $\{\mathbf{S}\}$, referred to as the

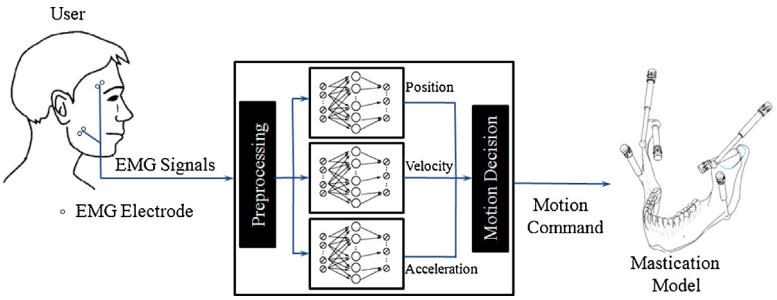

Fig. 7. Hybrid structure of an SEMG-based human mastication/robot interface.

mandible's rotation matrix ${}^{S}_{M}\mathbf{R}$, is defined using roll, pitch, and yaw angles γ, β, and α, respectively, as shown in Eq. (6).

$$ {}^{S}_{M}\mathbf{R} = \begin{bmatrix} c\gamma\, c\beta & c\gamma\, s\beta\, s\alpha - s\gamma\, c\alpha & c\gamma\, s\beta\, c\alpha + s\gamma\, s\alpha \\ s\gamma\, c\beta & s\gamma\, s\beta\, s\alpha + c\gamma\, c\alpha & s\gamma\, s\beta\, c\alpha - c\gamma\, s\alpha \\ -s\beta & c\beta\, s\alpha & c\beta\, c\alpha \end{bmatrix} \tag{6} $$

where $c\beta = \cos(\beta)$, $s(\beta) = \sin(\beta)$, and so on. According to Eq. (5), we have

$$ \begin{Bmatrix} S_x \\ S_y \\ S_z \end{Bmatrix} = \begin{Bmatrix} P_x \\ P_y \\ P_z \end{Bmatrix} + {}^{S}_{M}\mathbf{R} \begin{Bmatrix} b_x \\ b_y \\ b_z \end{Bmatrix} - \begin{Bmatrix} a_x \\ a_y \\ a_z \end{Bmatrix} \tag{7} $$

Therefore, the lengths of the actuators can be obtained as follows:

$$ S_i = ||\mathbf{s}_i|| = \sqrt{s_{ix}^2 + s_{iy}^2 + s_{iz}^2} = \sqrt{{}^{S}s_i^{T}\, {}^{S}S_i} \quad (i = 1,\ 2,\ \ldots,\ 6) \tag{8} $$

Eq. (8) provides the solution to the IKP. Position vectors ${}^{S}\mathbf{a}_i$ and ${}^{M}\mathbf{b}_i$ are fixed and known in the IKP. Therefore, by specifying the trajectory of the mandible, and knowing ${}^{S}\mathbf{P}$ and ${}^{S}_{M}\mathbf{R}$, Eq. (8) provides the required lengths of the six muscles.

The proposed mastication human robot is shown in Fig. 7. This system comprises two major parts: (1) SEMG-based kinematic pattern detection (EKP), and (2) motion decision (MD). In EKP, three TDANNs predict the corresponding position/orientation, velocity, and acceleration of subject's mandible, from the sampled preprocessed data $\mathrm{SEMG}_d(t)$, where $d = 1, 2, \ldots, n$. In MD, the required lengths and orientations of the six muscles are determined by using the EKP block estimate and the IKP solution (Eq. (5)). By predicting the subject's movement and solving the IKP, we provide applicable tools for controlling an SEMG-based masticatory robot.

3. Results

Sample SEMG (before preprocessing) and kinematic data obtained from one subject are shown in Fig. 8. During each trial, the subject opened and closed his jaw in the pre-specified time interval. Due to the symmetric role of the aforementioned muscles in the defined task, the data obtained from one temporalis and one masseter muscle were used for processing steps.

3.1. TDANN prediction of masticatory kinematics

The SEMG recording from one subject was used to assess the ability of three TDANNs to predict the position/orientation, velocity, and acceleration of the mandible (Fig. 9). The performance of the proposed method was evaluated with the validation dataset. The three rows represent (from top to bottom) the kinematic parameters of the x, z, and β variables. The three column panels represent (from left to right) position/orientation, velocity, and acceleration. Four input cases were chosen: SEMG signals of the temporalis and masseter muscles at different delays (with no output delay, using TDANN), and SEMG signals with output delays of 50, 100, and 150 ms (using AR-TDANN). Output delays were used to evaluate the efficiency of the proposed method in the case that cameras with different resolutions (in terms of fps) are employed. In general, the TDANN performed well in predicting each of the three kinematic parameters. However, adding output feedback (using AR-TDANN) significantly improved the outcome. Averages of the evaluation criteria (i.e., from Eqs. (2) to (4)) are shown in Table 1 for all subjects. These criteria were calculated for the training and validation stages. Each cell presents the RMSE, CC, and AAE results. In most cases, the velocity and acceleration predictions were less accurate than the position/orientation predictions. Because these two parameters were computed by numerical differentiation, larger error values

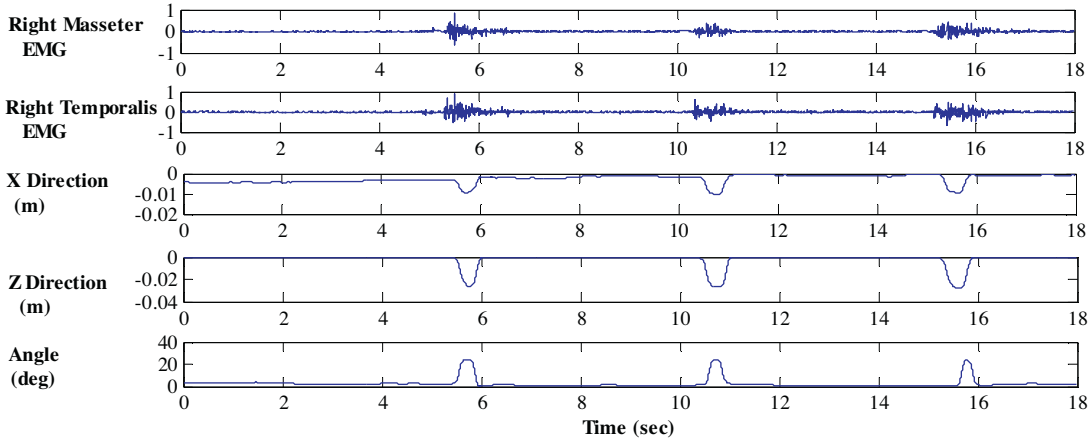

Fig. 8. Sample dataset recorded from one subject.

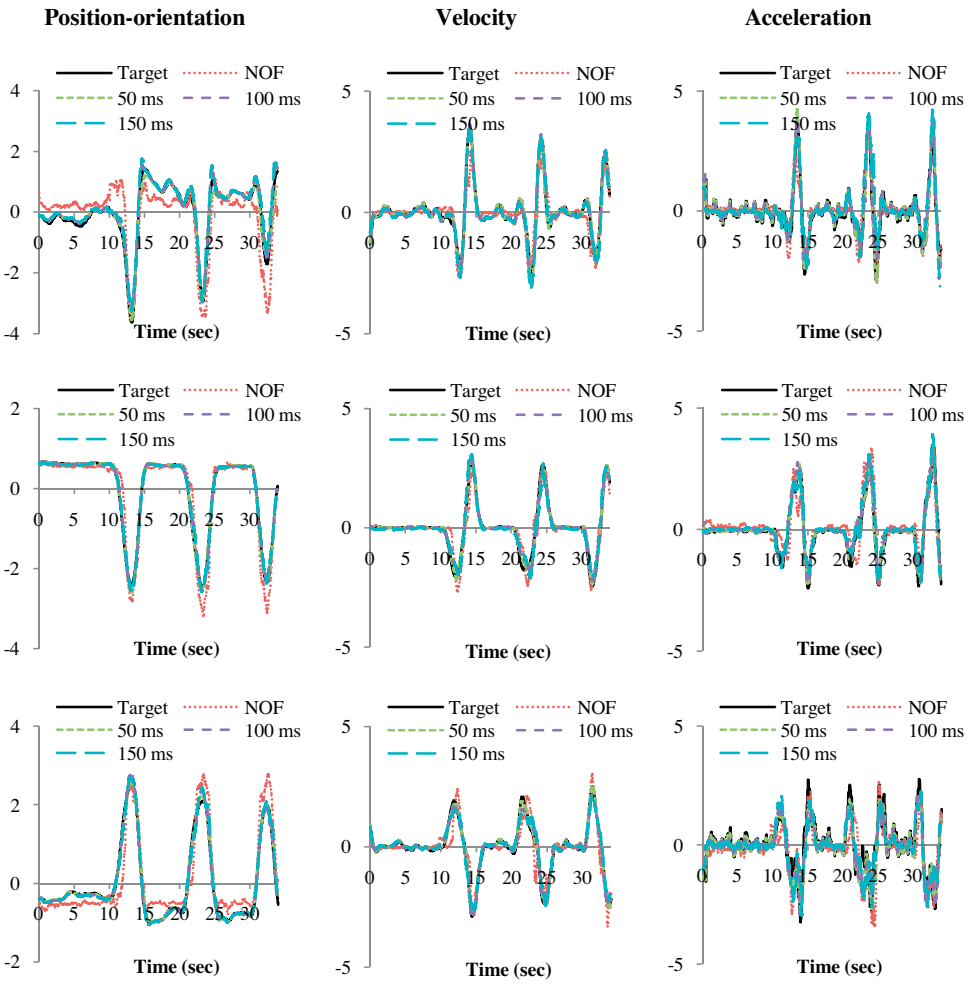

Fig. 9. Performance of TDANNs and AR-TDANNs in predicting three kinematic parameters (position/orientation, velocity, and acceleration). All inputs and output were normalized as *z*-scores. The three rows represent (from top to bottom) kinematic parameters for the *x*, *z*, and β variable, respectively.

were expected. Prediction was improved by considering output delays. As expected, a delay of 50 ms was the most effective for improving the model; however, including output delays of 100 or 150 ms also provided satisfactory results.

We investigated the efficiency of a TDANN (AR-TDANN) trained on signals obtained from one subject in predicting the output parameters for another subject. Fig. 10 presents the evaluation of network performance. Each bar in the figure represents the mean CC/AAE for predicting the dynamic parameters of maximum jaw opening/closing across all seven subjects, with the vertical bar indicating standard deviation. In general, the performance of the AR-TDANNs was superior to that of the TDANNs. The prediction error of position/orientation was less than the prediction error of velocity and acceleration. From this figure, it can be concluded that the identified models for position/orientation, velocity, and acceleration, trained on the data obtained from subject 2, can be appropriately generalized to other subjects. In all subjects, the prediction power of TDANN was significantly improved when an output delay of 50 ms was used. Fig. 10c demonstrates that the identified model for acceleration for each subject was not applicable to other subjects, due to the complexity of acceleration, except when an output delay of 50 ms was used.

Table 2 presents the mean RMSE, AAE, and CC values for the seven subjects, obtained through inter-subject validation of the developed models for TDANN and AR-TDANN. TDANN predicted mastication motions with reasonable accuracy when using recorded SEMG signals from mastication muscles. However, the results were significantly improved by employing the AR-TDANN architecture.

One-way ANOVA (analysis of variance) and multiple comparisons were performed on three groups of predictions (position/orientation, velocity and acceleration) to compare the performance of the models with NOF (no output feedback) and output feedback at 50, 100 and 150 ms delays. The analysis statistically verified significant for a *p*-value less than 0.05. The *p*-values for the three groups are shown in Table 3. Moreover, the box plot in Fig. 11 illustrates the range of the prediction %RMSE for cases NOF and 50–150 ms output delays. In general, it was concluded that the AR-TDANN gave lower %RMSE compared to TDANN. In other words, the error reduced from TDANN to AR-TDANN, with the output delay of 50 ms having the most significant reduction in %RMSE ($p < 0.0008$ for position/orientation, $p < 0.0003$ for velocity and $p < 2e{-}6$ for acceleration). Table 3 shows that a delay difference of 100 ms in the output feedback provides significant differences in the prediction accuracy, while this does not hold when the delay difference is reduced to 50 ms. We also investigated whether by employing the models with NOF or 50–150 ms output delays as feedback one of the target variables (*x*, *z*, and β variables) were predicted more accurately compared to the other two. In order to do this ANOVA was performed on the %RMSE values obtained after validation. Table 4 shows that almost all models did not performed significantly different (in the statistical sense) in predicting the target variables (and their derivatives).

Table 1
Mean RMSE, CC, AAE values for validation networks.

	Displacement		Velocity		Acceleration	
	Training	Validation	Training	Validation	Training	Validation
Sub. 1						
*NOF	36, 87, 0.3	59, 75, 0.5	39, 89, 0.3	43, 82, 0.4	16, 92, 0.2	61, 71, 0.4
OD 50 ms	0.7, 99, 0.04	0.7, 99, 0.05	3, 99, 0.09	4, 99, 0.1	4, 98, 0.1	6, 96, 0.1
OD 100 ms	2.9, 98, 0.1	2, 98, 0.1	9, 98, 0.1	10, 97, 0.1	12, 95, 0.2	16, 92, 0.2
OD 150 ms	2, 98, 0.1	2, 98, 0.1	9, 98, 0.1	10, 97, 0.1	10, 94, 0.2	25, 86, 0.3
Sub. 2						
*NOF	6, 96, 0.2	39, 78, 0.4	27, 85, 0.4	50, 72, 0.4	11, 94, 0.2	65, 65, 0.4
OD 50 ms	0.1, 99, 0.02	2, 98, 0.07	0.7, 99, 0.06	4, 98, 0.1	4, 98, 0.1	14, 92, 0.2
OD 100 ms	1, 99, 0.07	14, 95, 0.1	1.5, 99, 0.1	7, 95, 0.1	2.5, 99, 0.1	15, 92, 0.2
OD 150 ms	0.9, 99, 0.08	6, 96, 0.1	2, 98, 0.1	14, 92, 0.2	4, 98, 0.2	28, 84, 0.3
Sub. 3						
*NOF	63, 73, 0.5	64, 77, 0.5	33, 90, 0.3	58, 82, 0.5	46, 78, 0.5	53, 76, 0.5
OD 50 ms	5, 97, 0.1	39, 98, 0.09	10, 96, 0.2	10, 94, 0.2	31, 84, 0.3	30, 85, 0.3
OD 100 ms	8, 97, 0.1	6, 97, 0.1	24, 90, 0.3	22, 90, 0.2	93, 62, 0.6	65, 72, 0.4
OD 150 ms	19, 95, 0.2	10, 95, 0.1	29, 89, 0.3	31, 86, 0.3	75, 60, 0.6	96, 53, 0.6
Sub. 4						
*NOF	10, 94, 0.2	8, 96, 0.2	17, 91, 0.3	6, 97, 0.1	31, 84, 0.5	20, 91, 0.4
OD 50 ms	1.3, 99, 0.09	0.9, 99, 0.06	1.7, 99, 0.1	0.8, 99, 0.05	7, 96, 0.2	7, 96, 0.1
OD 100 ms	1, 99, 0.1	1, 99, 0.08	6, 97, 0.2	6, 96, 0.1	8.3, 95, 0.2	21, 88, 0.3
OD 150 ms	3, 98, 0.1	2, 98, 0.1	7, 96, 0.2	5, 97, 0.1	24, 93, 0.4	28, 84, 0.3
Sub. 5						
*NOF	11, 94, 0.3	33, 82, 0.4	9, 95, 0.2	41 (81) [0.3]	20, 91, 0.4	49, 76, 0.4
OD 50 ms	1.5, 99, 0.09	0.9, 99, 0.06	1.1, 99, 0.09	1, 99, 0.08	6, 96, 0.1	6, 96, 0.1
OD 100 ms	2.7, 98, 0.1	4.7, 97, 0.1	3, 98, 0.1	6, 97, 0.1	7, 96, 0.2	15, 94, 0.2
OD 150 ms	5, 97, 0.2	9, 94, 0.2	5, 97, 0.2	8, 96, 0.2	13, 92, 0.3	27, 85, 0.3
Sub. 6						
*NOF	3, 98, 0.1	24, 88, 0.3	3, 98, 0.1	25, 88, 0.3	18, 91, 0.3	38, 79, 0.4
OD 50 ms	0.1, 99, 0.02	0.9, 99, 0.05	0.4, 99, 0.04	0.8, 99, 0.05	59, 97, 0.1	6, 96, 0.1
OD 100 ms	0.2, 99, 0.03	1, 99, 0.06	1.2, 99, 0.08	2, 98, 0.1	9, 96, 0.2	11, 34, 0.2
OD 150 ms	0.4, 99, 0.05	2, 98, 0.09	1, 99, 0.1	4, 97, 0.1	12, 95, 0.2	27, 85, 0.3
Sub. 7						
*NOF	20, 90, 0.3	81, 62, 0.5	9, 95, 0.2	29, 88, 0.4	23, 88, 0.3	64, 77, 0.4
OD 50 ms	0.9, 99, 0.07	3, 98, 0.1	1.7, 99, 0.09	4, 97, 0.1	4, 98,0.1	11, 94, 0.2
OD 100 ms	3, 98, 0.1	5, 97, 0.1	3, 98, 0.1	6, 97, 0.1	8, 96, 0.2	41, 83, 0.4
OD 150 ms	4, 98, 0.1	8, 95, 0.2	12, 94, 0.2	15, 92, 0.2	15, 92, 0.2	15, 92, 0.2

* NOF: no output feedback (TDANN), OD: output delay (AR-TDANN).

Table 2
Mean RMSE, AAE and CC values for all subjects.

Method	Displacement			Velocity			Acceleration		
	Avg. RMSE	Avg. AAE	Avg. CC	Avg. RMSE	Avg. AAE	Avg. CC	Avg. RMSE	Avg. AAE	Avg. CC
TDANN									
*NOF	44 ± 25	0.4 ± 0.1	80 ± 10	36 ± 17	0.3 ± 0.1	84 ± 7	55 ± 9	04 ± 0.03	73 ± 4
ARTDANN									
OD 50 ms	1.9 ± 1.1	0.08 ± 0.02	99 ± 0.5	3.7 ± 3.2	0.1 ± 0.04	98 ± 1.6	11 ± 8	0.2 ± 0.06	94 ± 4
OD 100 ms	5.1 ± 4.4	0.1 ± 0.04	97 ± 1.3	7.9 ± 6.5	0.1 ± 0.05	96 ± 2.8	26 ± 19	0.3 ± 0.1	87 ± 7
OD 150 ms	6 ± 3.7	0.1 ± 0.05	97 + 1.7	12 ± 9	0.2 ± 0.07	94 ± 4	43 ± 30	0.4 + 0.1	80 ± 12

* NOF: no output feedback (TDANN), OD: output delay (AR-TDANN).

Table 3
p-Values for comparing the accuracy of all models.

		Displacement				Velocity				Acceleration			
		*NOF	50 ms	100 ms	150 ms	*NOF	50 ms	100 ms	150 ms	*NOF	50 ms	100 ms	150 ms
	*NOF	–	<8e−4	<0.002	<0.002	–	<3e−4	<0.002	<0.008	–	<2e−6	<0.005	<0.4
p-Value	50 ms	–	–	<0.09	<0.01	–	–	<0.1	<0.02	–	–	<0.09	<0.02
	100 ms	–	–	–	<0.5	–	–	–	<0.2	–	–	–	<0.2

* NOF: no output feedback, output delays of 50–150 ms.

Table 4
p-Values for comparing the accuracy of displacement, velocity and acceleration.

	*NOF			50 ms			100 ms			150 ms		
	Displacement	Velocity	Acceleration	Displacement	Velocity	Acceleration	Displacement	Velocity	Acceleration	Displacement	Velocity	Acceleration
p-Value	<0.006	<0.1	<0.2	<0.2	<0.3	<0.2	<0.3	<0.3	<0.3	<0.1	<0.3	<0.2

* NOF: no output feedback, output delays of 50–150 ms.

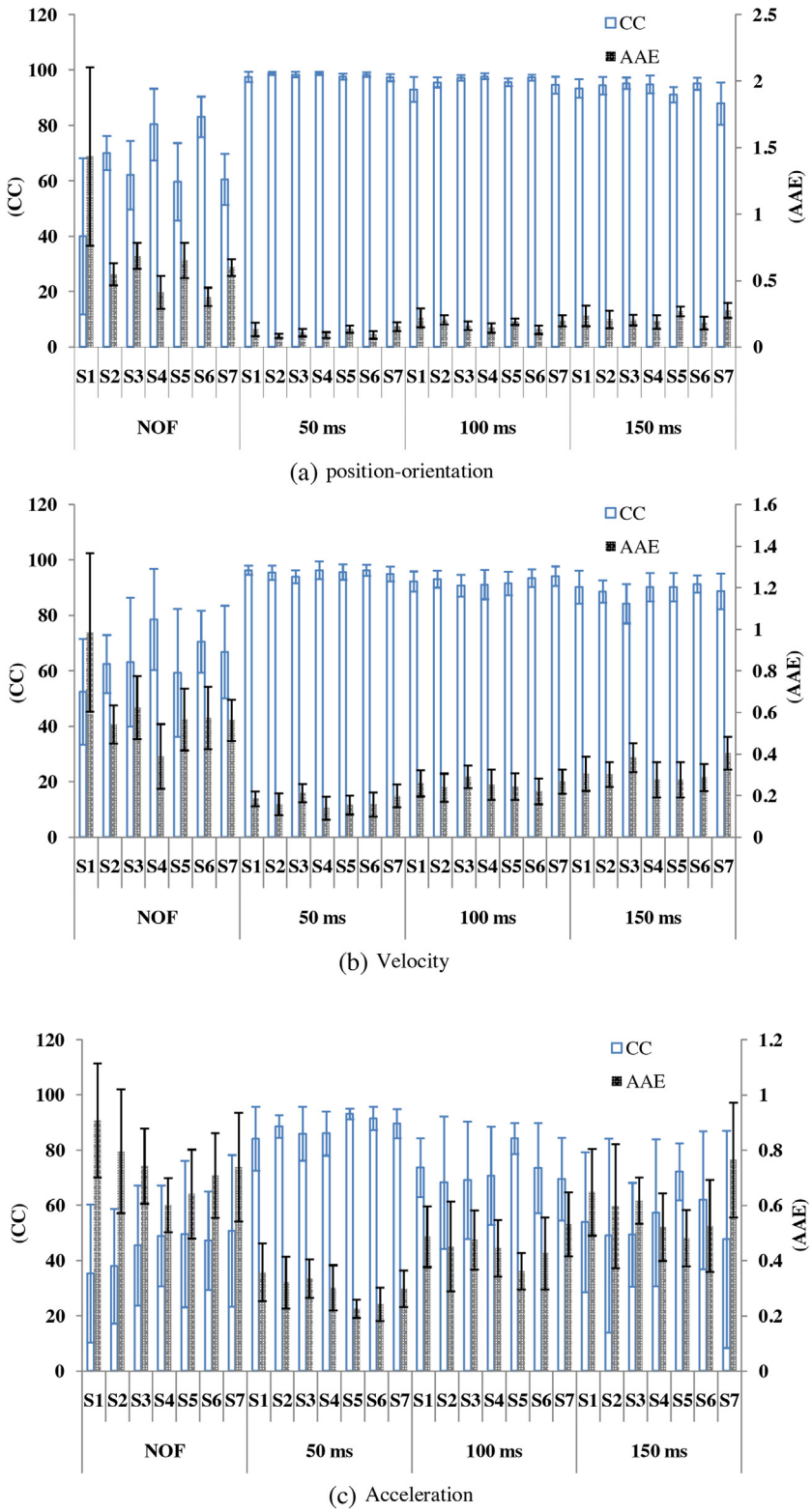

Fig. 10. Summary of CC and AAE values of TDANN of each subject's models to another subject. Each bar represents the average AAE and CC values for all subjects. Error bars indicate the standard deviation.

3.2. Case study of SEMG-based kinematic prediction

According to the results, considerable information can be obtained from SEMG recordings about the static position and dynamics of motion during mastication. An automatic control scheme might also be possible for the control of the mastication model. Based on the results above and Fig. 7, SEMG signals can be used to predict the length and orientation of each muscle during mastication by solving the IKP. For this purpose, the SEMG signal of subject 4 was employed as a case study. Considering the TDANN output of this subject as the input of the IKP (Eq. (5)), the required lengths and orientation of the actuators (muscles) were

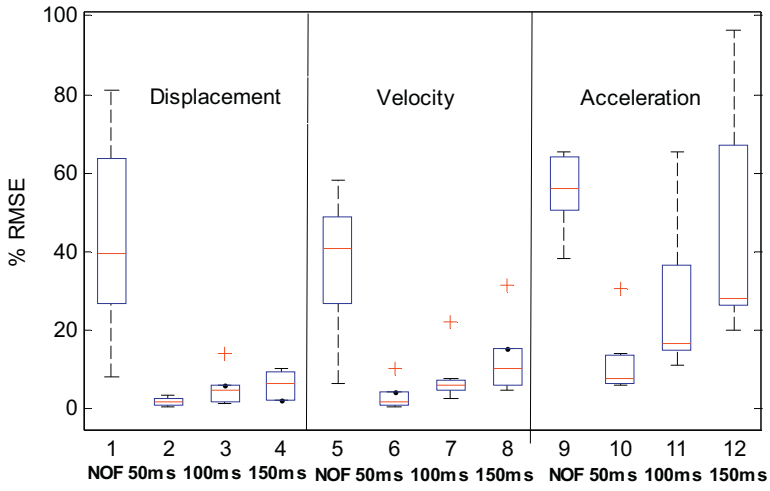

Fig. 11. One-way ANOVA box plot comparing %RMSE for NOF, 50 ms, 100 ms and 150 ms.

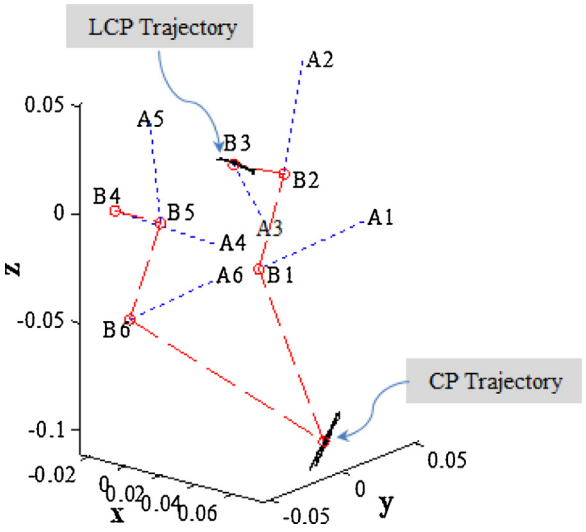

Fig. 12. Posture of the mastication muscles and mandible during clenching for subject 4. Trajectory of CP and LCP are shown. (For interpretation of the references to color in the text, the reader is referred to the web version of this article.)

computed. Representative posture variations, both orientation and position, during the trajectory and their IKP solutions are illustrated in Fig. 12. The blue dotted line and red dashed line correspond to the muscles and mandible, respectively (e.g., segment A_5B_5 represents the right temporalis muscle). Bold black lines show the paths of the CP and the left condyle point (LCP). Fig. 12 shows that this path can be obtained (in two or three dimensions) by the method suggested in the present study. The time-varying behavior of the muscle lengths, linear velocity, and linear acceleration are shown in Fig. 13 for one subject.

4. Discussion

The aim of this study was to develop an SEMG-based model by means of which jaw opening and closing during the mastication process can be reproduced. The results presented above indicate that if a gross prediction of the jaw motion is desired a TDANN can predict the trajectory with reasonable accuracy using only SEMG signals. The predictions are less accurate during maximum jaw opening. Accuracy compensation can be obtained by using the AR-TDANN structure (Fig. 9).

Other nonlinear system identification methods [32] could also be used in combination with GA for predicting the jaw motion from SEMG signals. However, the robust convergence properties of the backpropagation method and the relatively small number of unknown parameters to be estimated in TDANN/AR-TDANN made it an appropriate choice for modeling the underlying dynamics.

Generalization is one of the characteristics required for the developed model to be applicable for control purposes (e.g. masticatory robots with closed loop control systems). A recent study [6] suggested that the identified TDANN for one subject may not be valid for another subject. Discrepancies may be owing to differences between subjects in, for example, electrode positioning with respect to the motor points of the muscles, the amount of tissue between the electrodes and muscles, and characteristics of the muscles/muscle fibers [29]. In Fig. 10 we demonstrated that the models trained on the data obtained from one of the subjects could be appropriately generalized to other subjects. This observation suggests that these models are more comprehensive than previous ones. The improvement may be due to our use of an automatic method (GA) to determine the model architecture. Inter-subject variations of prediction accuracy could be owing to differences in jaw geometry, oral status, and other factors that were not considered in our model.

SEMG signals have previously been employed for recognizing intended motions of the musculoskeletal system with success [24,35,28]. However when predicting the natural movement and its moments is required inputs other than the SEMG signals are commonly adopted [23,34]. In this paper we demonstrated that including different delays of the recorded trajectory as inputs in the model provided significant improvement (in statistical sense) in the prediction ability of the proposed model (Table 3 and Fig. 11).

Numerous studies have evaluated the performance of the temporomandibular joint (TMJ) using the trajectory of condylar paths [11]. Studies have characterized the compound movement of the TMJ in two and three dimensions. Spoor [37] and Gallo et al. [1] used the screw axis model (also known as the finite helical axis model) to model TMJ movements in three dimensions. Grimes et al. [27] employed a tracking system and software with the screw displacement axis (SDA) model to perform a mathematical analysis of the movement of an object in three dimensions. They calculated rotation, translation, and the two- and three-dimensional charting of the condylar path. The muscle behavior could be approximated by harmonic series. In the current study it was possible to identify the path of each point in the mandible, the muscle orientation, and the muscle length during mastication movements by using

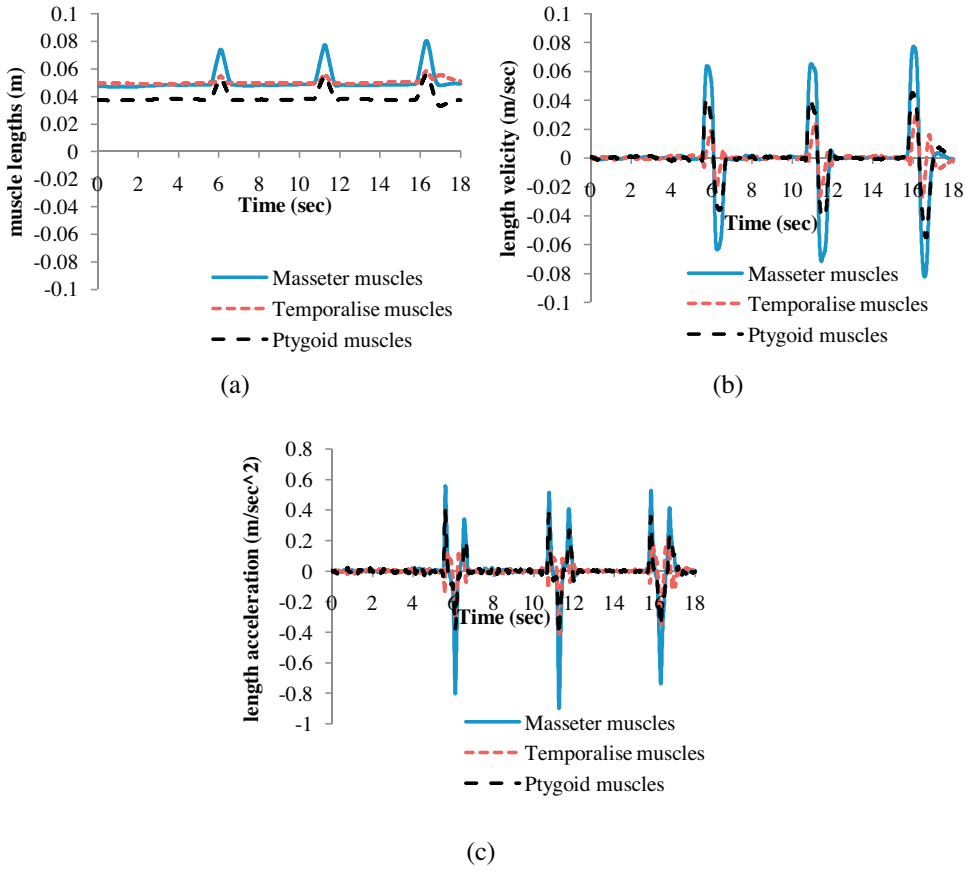

Fig. 13. Time-variations in (a) length, (b) linear velocity, and (c) linear acceleration during chewing.

the proposed hybrid structure. Although the kinematic motion parameters were estimated using only SEMG signals from the masseter and temporalis muscles, once the estimation is complete, the IKP can be solved to compute the time-varying length of all three muscles (Fig. 13).

This study was limited to clenching movements since considering the ethical issues we only used surface electrodes for recording the electrical activity of the muscles. Employing needle electrodes and recording the electrical activity of pterygoid muscles can provide the required tools for predicting lateral jaw motion during mastication, hence having a more realistic reproduction of the system under study. In that case the same techniques explained in this paper could easily accommodate a combination of the new muscles along with the ones employed in the current study.

5. Conclusion

EMG has been widely used as a control command for prostheses and powered exoskeleton robots. This paper considered whether recorded SEMG signals from voluntary muscles are sufficient for predicting the kinematics (position/orientation, velocity, and acceleration) of mandible motion in clenching movements. Two different methods, TDANN and AR-TDANN, were proposed. In general, the results showed that: (1) the TDANN and AR-TDANN methods are capable of providing reasonably accurate estimations of mastication motion, and (2) the SEMG signals contain important information about mastication movement. In all cases, the performance of AR-TDANN was better than that of TDANN. However, in the absence of motion sensors, TDANN would be sufficiently efficient for controlling masticatory robots.

The provided analysis will aid researchers in characterizing and investigating the mastication process, through the specification of SEMG signal patterns (e.g., muscle displacements) and the observation of the resulting mandible movement. Such models can provide clinical insight into the development of more effective rehabilitation therapies, and can aid in assessing the effects of an intervention. This methodology can be applied to any teleoperated robot or orthotic device (exoskeleton), either for rehabilitation or extension of human ability.

Acknowledgement

The work described in this paper was supported by a grant from the research office of Ferdowsi University of Mashhad, Mashhad, Iran.

References

[1] R.L. Airoldi, L.M. Gallo, S. Palla, Precision of the jaw tracking system Jaws 3D, J. Orofac. Pain 8 (1994) 155–164.
[2] A.T.C. Au, R.F. Kirsch, EMG-based prediction of shoulder and elbow kinematics in able-bodied and spinal cord injured individuals, IEEE Trans. Rehabil. Eng. 8 (4) (2000) 471–480.
[3] A. Balbinot, G. Favieiro, A neuro-fuzzy system for characterization of arm movements, Sensors 13 (2013) 2613–2630.
[4] J. Barbenel, The mechanics of the temporomandibular joint – a theoretical and electromyographical study, J. Oral Rehabil. 1 (1) (1974) 19–27.
[5] D. Braxton, C. Dauchel, W.E. Brown, Association between chewing efficiency and mastication patterns for meat, and influence on tenderness perception, Food Qual. Prefer. 7 (3–4) (1996) 217–223.
[6] W.E. Brown, K.R. Langley, L. Mioche, S. Marie, S. Gerault, D. Braxton, Individuality of understanding and assessment of sensory attributes of foods, in particular, tenderness of meat, Food Qual. Prefer. 7 (3–4) (1996) 205–216.

[7] W.E. Brown, D. Braxton, Dynamics of food breakdown during eating in relation to perceptions of texture and preference: a study on biscuits, Food Qual. Prefer. 11 (4) (2000) 259–267.
[8] N. Bu, M. Okamoto, A. Tsuji, hybrid motion classification approach for EMG-based human–robot interfaces using Bayesian and neural networks, IEEE Trans. Robot. 25 (3) (2009) 502–511.
[9] N. Bu, T. Tsuji, O. Fukuda, EMG-based motion discrimination using a novel recurrent neural network, Int. J. Intell. Syst. 21 (2) (2003) 113–126.
[10] G. Cheron, J.P. Draye, M. Brougeios, G. Libert, A dynamic neural network identification of electromyography and arm trajectory relationship during complex movements, IEEE Trans. Biomed. Eng. 43 (1995) 552–558.
[11] J.A. Clayton, A pantographic reproducibility index for use in diagnosing TMJ function: a report on research, J. Pros. Dent. 54 (1985) 827–831.
[12] C.J. De Luca, L.D. Gilmore, M. Kuznetsov, S.H. Roy, Filtering the surface EMG signal: movement artifact and baseline noise contamination, J. Biomech. 43 (2010) 1573–1579.
[13] O. Fukuda, T. Tsuji, M. Kaneko, A. Ohtsuka, A human-assisting manipulator teleoperated by EMG signals and arm motions, IEEE Trans. Robot. Autom. 19 (2) (2003) 210–222.
[14] O. Fukuda, T. Tsuji, M. Kaneko, A. Ohtsuka, A human-assisting manipulator teleoperated by EMG signals and arm motions, IEEE Trans. Robot. 19 (2) (2003) 210–222.
[15] R. González, I. Montoya, J. Cárcel, Review: the use of electromyography on food texture assessment, Food Sci. Technol. Int. 7 (6) (2001) 461–471.
[16] D. Graupe, J. Magnussen, A.A.M. Beex, A microprocessor system for multifunctional control of upper limb prostheses via myoelectric signal identification, IEEE Trans. Autom. Control 23 (4) (1978) 538–544.
[17] J.R. Green, Orofacial movement analysis in infants and young children: new opportunities in speech studies, Standard 2 (2002) 1–3.
[18] B. Hudgins, P. Parker, R.N. Scott, A new strategy for multifunction myoelectric control, IEEE Trans. Biomed. Eng. 40 (1) (1993) 82–94.
[19] X.L. Hu, K.Y. Tong, R. Song, X.J. Zheng, K.H. Lui, W.W. Leung, S. Ng, S.S. Au-Yeung, Quantitative evaluation of motor functional recovery process in chronic stroke patients during robot-assisted wrist training, J. Electromyogr. Kinesiol. 19 (4) (2009) 639–650.
[20] Y. Ioannides, J. Seers, M. Defenez, C. Raithatha, M.S. Howarth, A. Smith, E.K. Kemsleys, Electromyography of the masticatory muscles can detect variation in the mechanical and sensory properties of apples, Food Qual. Prefer. 20 (3) (2009) 203–215.
[21] F.R. Jack, J.R. Piggott, A. Paterson, Relationships between electromyography, sensory and instrumental measures of cheddar cheese texture, J. Food Sci. 58 (6) (1993) 1313–1317.
[22] W.J. Kang, J.R. Shiu, C.K. Cheng, J.S. Lai, H.W. Tsao, T.S. Kuo, The application of cepstral coefficients and maximum likelihood method in EMG pattern recognition, IEEE Trans. Biomed. Eng. 42 (8) (1995) 777–785.
[23] W. Karwowski, et al., A fuzzy relational rule network modeling of electromyographical activity of trunk muscles in manual lifting based on trunk angels, moments, pelvic tilt and rotation angles, Int. J. Ind. Ergon. 36 (10) (2006) 847–859.
[24] M. Khezri, J. Mehran, A neuro-fuzzy inference system for sEMG-based identification of hand motion commands, IEEE Trans. Ind. Electron. 58 (5) (2011) 1952–1960.
[25] M.F. Kelly, P. Parker, R.N. Scott, The application of neural networks to myoelectric signal analysis: a preliminary study, IEEE Trans. Biomed. Eng. 37 (3) (1990) 221–230.
[26] E.K. Kemsley, M. Defernez, J.C. Sprunt, A.C. Smith, Electromyographic responses to prescribed mastication, J. Electromyogr. Kinesiol. 13 (2) (2003) 197–207.
[27] S.K. Lehman-Grimes, A Review of Temporomandibular Disorder and An Analysis of Mandibular Motion (Master of dental science thesis), The University of Tennessee, 2005.
[28] R.T. Lauer, B.T. Smith, R.R. Betz, Application of a neuro-fuzzy network for gait event detection using electromyography in the child with cerebral palsy, IEEE Trans. Biomed. Eng. 52 (9) (2005) 1532–1540.
[29] L. Ljung, System Identification, John Wiley & Sons Inc., 1999.
[30] L. Lucas, M. Dicicco, Y. Matsuoka, An EMG-controlled hand exoskeleton for natural pinching, J. Robot. Mechatron. 16 (5) (2004) 482–488.
[31] B. May, S. Saha, M. Saltzman, A three-dimensional mathematical model of temporomandibular joint loading, Clin. Biomech. 16 (6) (2001) 489–495.
[32] V.Z. Marmarelis, Nonlinear Dynamic Modeling of Physiological Systems, vol. 10, John Wiley & Sons, 2004.
[33] F. Mobasser, K. Hashtrudi-Zaad, A comparative approach to hand force estimation using artificial neural networks, Biomed. Eng. Comput. Biol. Insights 4 (2012) 1–15.
[34] F. Mobasser, J. Mikael Eklund, K. Hashtrudi-Zaad, Estimation of elbow-induced wrist force with EMG signals using fast orthogonal search, IEEE Trans. Biomed. Eng. 54 (4) (2007) 683–693.
[35] J. Sh, et al., SEMG-based hand motion recognition using cumulative residual entropy and extreme learning machine, Med. Biol. Eng. Comput. 51 (4) (2013) 417–427.
[36] H.J. Smit, E.K. Kemsley, H.S. Tapp, J.K. Henry, Does prolonged chewing reduce food intake? Fletcherism revisited, Appetite 57 (1) (2011) 295–298.
[37] C.W. Spoor, Explanation, verification and application of the helical axis error propagation formulas, Hum. Mov. Sci. 3 (1984) 95–117.
[38] D. Staudenmann, K. Roeleveld, D. Stegeman, J. van Dieën, Methodological aspects of SEMG recordings for force estimation – a tutorial and review, J. Electromyogr. Kinesiol. 20 (3) (2010) 375–387.
[39] H. Takanobu, K. Ohtsuki, A. Takanishi, M. Ohnishi, A. Okino, Jaw training robot and its clinical results, in: International Conference on Advanced Intelligent Mechatronics, 2003, pp. 932–937.
[40] J.D. Torrance, Kinematics, Motion Control and Force Estimation of a Chewing Robot of 6RSS Parallel Mechanism (Ph.D. thesis), Massy University, Palmerston North, New Zealand, 2011.
[41] T. Tsuji, H. Ichinobe, K. Ito, M. Nagamachi, Discrimination of forearm motions from EMG signals by error back propagation typed neural network using entropy, Trans. Soc. Instrum. Control Eng. 29 (3) (1993) 1213–1220.
[42] T. Tsuji, O. Fukuda, M. Kaneko, K. Ito, Pattern classification of time-series EMG signals using neural networks, Int. J. Adapt. Control Signal Process. 14 (2000) 829–848.
[43] E.M. Wilson, J.R. Green, The development of jaw motion for mastication, Early Hum. Dev. 85 (5) (2009) 303–311.
[44] J.M. Wu, Multilayer Potts perceptrons with Levenberg–Marquardt learning, IEEE Trans. Neural Netw. 19 (2008) 2032–2043.
[45] W. Xu, J.E. Bronlund, Mastication Robots: Biological Inspiration to Implementation, Springer-Verlag Berlin Heidelberg Press, 2010.
[46] M. Zecca, S. Micera, M.C. Carrozza, P. Dario, Control of multifunctional prosthetic hands by processing the electromyographic signal, Crit. Rev. Biomed. Eng. 30 (4–6) (2002) 459–485.
[47] U. Posselt, Movement areas of the mandible, J. Pros. Dent. 7 (1957) 375–385.